DMD Fast Forward. Published on April 2, 2007 as doi:10.1124/dmd.106.014597

DMD#14597

Biotransformation of 6-Methoxy-3- (3',4',5'-trimethoxy- benzoyl)-1*H*-indole (BPR0L075), A Novel Antimicrotubule Agent, By Mouse, Rat, Dog And Human Liver Microsomes

HSIEN-TSUNG YAO, YU-SHAN WU, YI-WEI CHANG, HSING-PANG HSIEH, WEI-CHENG CHEN, SHIH-JUNG LAN, CHIUNG-TONG CHEN, YU-SHENG CHAO, LING CHANG, HSU-YI SUN, TENG-KUANG YEH*

Division of Biotechnology and Pharmaceutical Research, National Health Research Institutes, 35, Keyan Road, Zhunan Town, Miaoli County, Taiwan, R.O.C.

DMD Fast Forward. Published on April 2, 2007 as DOI: 10.1124/dmd.106.014597
This article has not been copyedited and formatted. The final version may differ from this version.

Running title: Biotransformation of BPR0L075 in Liver Microsomes

Corresponding author: Dr. Teng-Kuang Yeh

Division of Biotechnology and Pharmaceutical Research

National Health Research Institutes

35 Keyan Road, Zhunan Town

Miaoli County, Taiwan

Tel: 886-37-246-166 ext.35757

Fax: 886-37-586-456

The number of text pages: 17

The number of tables: 2

The number of figures: 7

The number of references: 4

The number of words in Abstract: 257

The number of words in Introduction: 236

The number of words in Discussion: 1336

Abbreviations:

P450, cytochrome P450; BPR0L075, 6-methoxy-3- (3',4',5'-trimethoxy-benzoyl)-1*H*-indole ; LC/MS, liquid chromatography/mass spectrometry; LC/MS/MS, liquid chromatography tandem mass spectrometry

DMD Fast Forward. Published on April 2, 2007 as DOI: 10.1124/dmd.106.014597
This article has not been copyedited and formatted. The final version may differ from this version.

ABSTRACT

6-Methoxy-3- (3',4',5'-trimethoxy- benzoyl)-1*H*-indole (BPR0L075) is a novel synthetic indole compound with microtubule binding activity. Incubation of BPR0L075 with mouse, rat, dog and human liver microsomes in the presence of NADPH resulted in the formation of six metabolites. LC-MS/MS and comparison with the synthetic reference standards identified two metabolites (M1 and M5) as the products derived from hydroxylation on the indole moiety of the molecule. M3 was also identified as a product derived from hydroxylation, but the structure of this metabolite was not identified due to lack of reference standard. M2, M4 and M6 were identified as the products derived from O-demethylation. M2, 6-desmethyl-BPR0L075, was the major metabolite formed by the liver microsomes of the four species. No qualitative species-difference on the metabolism of BPR0L075 was observed. There was quantitative species-difference on the metabolism of BPR0L075 among the four species. While mouse and rat liver microsomes metabolized BPR0L075 predominantly via O-demethylation, dog liver microsomes metabolized BPR0L075 by O-demethylation and hydroxylation to about the same extent. The rank order of intrinsic clearance rates for the conversion of BPR0L075 to 6-desmethyl-BPR0L075 was mouse > rat > human > dog. Incubation of BPR0L075 with baculovirus-insect cell-expressed human CYP isozymes showed that CYP 1A2, 2C9, 2C19, 2D6, 2E1 and 3A4 all catalyzed the O-demethylation and hydroxylation of BPR0L075 but to a different degree. Among the six CYP isozymes tested, CYP 1A2 and 2D6 were most active on catalyzing the metabolism of BPR0L075. CYP 1A2 catalyzed mainly the formation of M1, M2 and M3. M2 was the predominant metabolite formed by CYP 2D6.

DMD Fast Forward. Published on April 2, 2007 as DOI: 10.1124/dmd.106.014597
This article has not been copyedited and formatted. The final version may differ from this version.

INTRODUCTION

6-Methoxy-3-(3',4',5'-trimethoxybenzoyl)-1*H*-indole (BPR0L075), is a new synthetic heterocyclic analogue of Combretastatin A-4 that is a naturally occurring stilbene derived from the South African tree *Combretum caffrum*. It exerts potent antitumor and antimitotic activities. The mechanism of action of BPR0L075 is known to inhibit tubulin polymerization by binding to tubulin at the colchicine-binding site. BPR0L075 showed the broad spectrum *in vitro* antitumor activity against a variety of human tumor cell lines including leukemia, glioblastoma, breast, gastric, colorectal and liver cancer cells. It also demonstrated potent activity against the growth of human cervical carcinoma KB and human gastric carcinoma MKN-45 xenografts (Kuo et al., 2004). BPR0L075 is currently undergoing preclinical investigation for the treatment of cancers.

In general, during drug discovery stage, one of the essential components is to optimize the absorption, distribution, metabolism, excretion and toxicity properties of the investigational compounds in order to reduce the attrition rate due to poor pharmacokinetic properties (Kerms, 2001). Knowledge of the metabolic fate of a compound is important because it affects clearance, half-life and oral bioavailability and governs the outcome of pharmacodynamic and toxicological observations (Hop et al., 2002). Thus, one of the primary roles in early preclinical investigations is to compare the metabolic fate of the compound among different species to provide the vital information for lead optimization as well as for toxicological assessment.

This study investigated the metabolic fate of BPR0L075 in mouse, rat, dog and human liver microsomes.

DMD Fast Forward. Published on April 2, 2007 as DOI: 10.1124/dmd.106.014597
This article has not been copyedited and formatted. The final version may differ from this version.

MATERIALS AND METHODS

Chemicals, Microsomes and Human CYP Isozymes

BPR0L075 and five putative metabolites, 5–hydroxyl–6-methoxy-3-(3',4',5'-trimethoxybenzoyl)indole (5-hydroxyl-BPR0L075) , 6-hydroxy-3-(3',4',5'-trimethoxybenzoyl) indole (6- desmethyl-BPR0L075; BPR0L082), 6-methoxy-3-(4'-hydroxy -3',5'-methoxybenzoyl)indole (4'-desmethyl-BPR0L075), 7-hydroxyl –6 –methoxy–3-(3',4',5'-trimethoxybenzoyl)indole (7-hydroxy -BPR0L075), 6-methoxy–3-(3'-hydroxy-4',5'-methoxybenzoyl)indole (3'-desmethyl-BPR0L075) and 6–ethoxy–3- (3',4',5'-trimethoxy-benzoyl)– 7-azaindole (BPR0L187) were synthesized in The Division of Biotechnology and Pharmaceutical Research, National Health Research Institutes, Zhunan, Miaoli County, Taiwan, ROC. NADPH was obtained from Sigma Chemical Co. (St Louis, MO, USA). Pooled liver microsomes from humans (male and female), male mice, male rats, and male dogs and human CYP enzymes (Supersomes) from baculovirus-insect cell-expressed human CYP1A2, 2C9, 2C19, 2D6, 2E1 and 3A4 containing cytochrome P450 reductase were purchased from BD Gentest (Woburn, MA, USA). All other chemicals were of reagent grade and were obtained commercially.

Incubation of BPR0L075 with Mouse, Rat, Dog and Human Liver Microsomes

The incubation mixture, in 84 mM potassium phosphate buffer (pH 7.4), consisted of: magnesium chloride, 3 mM; liver microsomal proteins, 1 mg/mL; NADPH, 3 mM and BPR0L075, 20 μM. The concentration of methanol (used for dissolving the substrate) was 1% (v/v). Total volume of incubation was 500 μL. Incubation was carried out aerobically at 37 ^{o}C with constant shaking in a test tube placed on a temperature-controlled heating block. Reaction was started by the addition of NADPH

DMD Fast Forward. Published on April 2, 2007 as DOI: 10.1124/dmd.106.014597
This article has not been copyedited and formatted. The final version may differ from this version.

after pre-incubating the reaction mixture (without NADPH) for 5 min at 37 ^{o}C. The incubation mixture without NADPH was used as the blank control. At 60 min after the start of reaction, the incubation mixture was mixed with 1 mL of ice-cold acetonitrile to terminate the reaction. The sample was then transferred to a centrifuge tube, vortexed and centrifuged at 20,800 × g for 20 min at room temperature. The supernatant was transferred to a separate tube and evaporated to dryness under nitrogen. The residues were dissolved in 0.1 mL of 40% acetonitrile in water. An aliquot (10 μL) of the reconstituted solution was then analyzed by LC/MS and LC/MS/MS for BPR0L075 and its metabolites.

Incubation of BPR0L075 with Baculovirus-insect cell-expressed Human CYP Isozymes

The incubation system was the same as those applied to the liver microsomal incubations with the exception that microsomes were replaced by baculovirus-insect cell-expressed human CYP1A2, 2C9, 2C19, 2D6, 2E1 and 3A4. The enzyme concentration in the incubation system was 100 pmol/mL. The total volume of incubation was 200 μL. After 60 min of incubation, the incubation mixture was mixed with 200 μL of ice-cold acetonitrile to terminate the reaction. The sample was then vortexed and centrifuged at 20,800$\times g$ for 20 min at room temperature. An aliquot (20 μL) of the supernatant was then analyzed by LC/MS and LC/MS/MS for BPR0L075 and its metabolites.

Kinetic Analysis of BPR0L075 Metabolism

In the kinetic experiments, eight concentrations of BPR0L075 (2-250 μM) were incubated in triplicate with mouse, rat, dog and human liver microsomes. The incubation conditions were the same as those described above except that the microsomal protein concentration was 0.5 mg/mL and the total volume of incubation

DMD Fast Forward. Published on April 2, 2007 as DOI: 10.1124/dmd.106.014597
This article has not been copyedited and formatted. The final version may differ from this version.

was 200 μL. The reaction was started by the addition of 20 μL of 30 mM NADPH in phosphate buffer. At 10 min after the start of reaction, 100 μL of each incubation mixture was taken and mixed with 100 μL of ice-cold acetonitrile containing the internal standard (BPR0L187; 200 ng/mL) to stop the reaction. The sample was then vortexed and centrifuged at 20,800$\times g$ for 20 min at room temperature. An aliquot (10 μL) of the supernatant was used for analysis of the formation of 6-desmethyl-BPR0L075 (BPR0L082) by LC/MS. The amount of formed 6-desmethyl-BPR0L075 was determined by comparing the peak area ratio of the testing samples with that of a sample containing a known concentration of the metabolite (BPR0L082) in microsomes incubated in the absence of NADPH.

LC-MS and LC-MS/MS Analyses

LC-MS was carried out with an Agilent 1100 Series LC System.equipped with an UV detector (Palo Alto, CA, USA). An Agilent Extend-C_{18} reverse-phase column (5 μm, 250 × 4.6 mm) was used. Mobile phase consisted of 10 mM ammonium acetate containing 0.1% of formic acid (Solvent A) and acetonitrile (Solvent B). The flow rate was 0.5 mL/min. Total running time was 60 min. The gradient system used to separate BPR0L075 and its metabolites was: 30%B (0-5 min), 30%B to 70%B (5-45 min), 70%B (45-50 min), 70%B to 30%B (50-60 min). The column temperature was 25°C. The effluent was monitored using a UV detector set at 286 nm and a mass spectrometer operating in the positive ion mode over the m/z range 200-600.

For the determination of 6-desmethyl-BPR0L075 (BPR0L082) formation in kinetic experiment, LC-MS was carried out with an Agilent Zorbax Eclipse XDB-C_8 reverse-phase column (5 μm, 150 × 3.0 mm). Mobile phase (Solvent A and B), flow rate and column temperature were the same as those described above. The gradient system used to separate 6-desmethyl-BPR0L075 and BPR0L187 (internal standard)

was: 30%B to 98%B (0-5 min), 98%B (5-7 min), 98%B to 30%B (7-10 min) and 30%B (10-14 min). The retention times of 6-desmethyl-BPR0L075/BPR0L187 were 4.8/6.4 min. Ions representing the $(M+H)^+$ species for both the metabolite and internal standard (IS) were selected and the peak areas were measured.

LC-MS/MS was carried out with an Agilent 1100 Series LC System (Palo Alto, CA, USA) and an AB Sciex API 3000 tandem mass spectrometer equipped with an electrospray ion in the positive ion mode (Applied Biosystems, Foster City, CA, USA). The source and desolvation temperature were held at 400^{o}C. The molecular ions of the analytes were extracted and fragmented by collision-induced dissociation. Nitrogen was used as the collision gas. The collision energy was 33V. Product ions were scanned in the m/z range 100-400. The analytical data were processed by Analyst software (version 1.4).

Data Analysis

Nonlinear regression analysis, $V=V_{max}S/(K_m+S)$, was used to describe the kinetics of biotransformation of BPR0L075 to 6-desmethyl-BPR0L075 in liver microsomes of the four species and was fitted to the untransformed data (Enzyme Kinetics, version 1.1, SPSS Science, Chicago, IL, USA). V is the velocity of the reaction at substrate concentration [S]; V_{max} is the maximum velocity; K_m is the substrate concentration at which the reaction velocity is 50% of V_{max}. The intrinsic clearance (Cl_{int}) was calculated as V_{max}/K_m.

DMD Fast Forward. Published on April 2, 2007 as DOI: 10.1124/dmd.106.014597
This article has not been copyedited and formatted. The final version may differ from this version.

RESULTS AND DISSCUSSION

Identification of Metabolites in Human Liver Microsomal Incubation

Figure 1 shows the total ion and representative extracted ion chromatograms of the acetonitrile extract of BPR0L075 incubated with human liver microsomes in the presence of NADPH. In addition to the unchanged BPR0L075, six metabolites were detected. Three of the six metabolites (M1, M3 and M5) showed the $(M+H)^+$ ion at m/z 358 which was 16 amu higher than that of the parent compound (342 amu) suggesting the addition of an oxygen atom to the molecule. The other three metabolites (M2, M4 and M6) showed the $(M+H)^+$ ion at m/z 328 which was 14 amu lower than that of the parent compound suggesting the loss of a CH_2 group from the molecule. Thus, Metabolites M1, M3 and M5 were tentatively identified as the metabolites derived from hydroxylation of BPR0L075 and metabolites M2, M4 and M6 as the metabolites derived from demethylation of BPR0L075.

The compound with a retention time of 28.5 min had the same retention time, the $(M+H)^+$ ion at m/z 342 and the fragmentation pattern of BPR0L075 standard. It was thus identified as the unchanged parent compound. The LC-MS/MS fragmentation pattern of BPR0L075 showed two prominent diagnostic fragment ions at m/z 195 and 174 (Figure 2).

M2, the major metabolite, had the $[M+H]^+$ ion at *m/z* 328 which was 14 amu lower than that of BPR0L075 suggesting the loss of a CH_2 group and was thus identified as a product of O-demethylation. LC-MS/MS of M2 yielded two fragment ions at m/z 195 and 160 (Figure 2). Compared to BPR0L075, the fragment ion at m/z 195 indicated that the methoxyl groups on the phenyl ring remained intact. The fragment ion at m/z 160 was 14 amu lower than that of the corresponding fragment

DMD Fast Forward. Published on April 2, 2007 as DOI: 10.1124/dmd.106.014597
This article has not been copyedited and formatted. The final version may differ from this version.

ion at m/z 174 of BPR0L075 standard suggesting that the demethylation reaction took place at the methoxyl group on the 6-position of the indole moiety. M2 had the same retention time, $(M+H)^+$ ion and fragmentation pattern of BPR0L082 standard (6-desmethyl-BPR0L075) and was thus identified as 6-desmethyl-BPR0L075.

M4 and M6 both had the $[M+H]^+$ ions at *m/z* 328 suggesting that they were also derived from O-demethylation of BPR0L075. Both M4 and M6 yielded the diagnostic fragment ions at m/z 174 and 181 (Figure 2) suggesting that the methoxyl group at the 6-position of the indole moiety remained intact and that O-demethylation occurred at the methoxyl groups on the phenyl ring. M4 and M6 showed the same retention times, $(M+H)^+$ and fragment ions of the synthetic 4'-desmethyl-BPR0L075 and 3'-desmethyl-BPR0L075 standards, respectively. Thus, they were identified as the metabolites derived from O-demethylation at the 4'- and 3'- positions on the phenyl moiety of the molecule, respectively.

M1, M3 and M5 all had the $[M+H]^+$ ion at *m/z* 358 which was 16 amu higher than that of the parent compound suggesting that an oxygen atom was inserted to the molecule of BPR0L075. The LC-MS/MS fragmentation pattern of the three metabolites all yielded the diagnostic fragment ions at m/z 195 and 190 indicating that the oxygen atom was inserted to the indole moiety of the molecule (Figure 2). M1 and M5 showed the same retention times, $(M+H)^+$ and fragment ions of the synthetic 5-hydroxyl-BPR0L075 and 7-hydroxyl-BPR0L075 standards, respectively. Thus, they were identified as the metabolites derived from hydroxylation at the 5- and 7-positions on the indole moiety of the molecule, respectively. The LC-MS/MS data showed that M3 also was a hydroxylation product of BPR0L075 with an oxygen atom being inserted to the indole moiety of the molecule. However, the reference standard was not synthesized due to technical reason. Thus, the position of hydroxylation of

DMD Fast Forward. Published on April 2, 2007 as DOI: 10.1124/dmd.106.014597
This article has not been copyedited and formatted. The final version may differ from this version.

M3 remains unknown.

Metabolism of BPR0L075 in Mouse, Rat, Dog and Human Liver Microsomes

To compare the metabolic fate of BPR0L075 across the species, BPR0L075 was separately incubated with mouse, rat and dog liver microsomes under the same conditions applied to human liver microsomes. The incubation mixtures were then extracted and analyzed for metabolites by the same LC-MS and LC-MS/MS methods applied to the human liver microsomal incubation.

Figure 3 shows the total ion and representative extracted ion chromatograms of the acetonitrile extract of BPR0L075 incubated with mouse, rat, dog and human liver microsomes in the presence of NADPH. Similar to the results obtained from the incubation of human liver microsomes, three hydroxylated metabolites of BPR0L075 (M1, M3 and M5) and three O-demethylated metabolites of BPR0L075 (M2, M4 and M6) were also presented in the incubations of mouse, rat and dog liver microsomes. Figure 4 shows the LC-UV chromatograms of the acetonitrile extract of BPR0L075 incubated with the liver microsomes of the four species. Table 1 shows the retention time, $(M+H)^+$ and major fragment ions, and the percent distribution of BPR0L075 and the metabolites in the liver microsomal incubations of the four species. The percent of metabolite formation was estimated based on the UV absorption and the assumption that all metabolites had the same extinction coefficient of the parent compound at 286 nm. The results showed that BPR0L075 was mainly metabolized by O-demethylation and hydroxylation in the liver microsomes of the four species. All six metabolites identified in the human liver microsomal incubation were also detected in the incubations of mouse, rat and dog liver microsomes. However, quantitative differences on the metabolism of BPR0L075 in the liver microsomes of the four species were observed. While mouse and rat liver microsomes metabolized

BPR0L075 predominantly via O-demethylation, dog liver microsomes metabolized BPR0L075 by O-demethylation and hydroxylation to about the same extent. The metabolic profile of BPR0L075 in human liver microsomes appears to be in between mouse and rat and dog liver microsomes (Table 1). Figure 5 depicts the proposed metabolic pathways of BPR0L075 in the liver microsomes of the four species.

Metabolism of BPR0L075 by Individual Human CYP Isozymes

BPR0L075 was separately incubated with baculovirus-insect cell-expressed human CYP 1A2, 2C9, 2C19, 2D6, 2E1 and 3A4 to determine the metabolic reactions of BPR0L075 catalyzed by individual CYP isozymes. After the incubation, the incubation mixtures were extracted and analyzed by LC-MS and LC-MS/MS for the formation of metabolites. Figure 6 shows the TIC and selectively extracted ion (at m/z 358 and 328 amu) chromatograms of the incubation of each CYP isozyme. The results showed that all six tested CYP isozymes catalyzed both the hydroxylation and O-demethylation of BPR0L075, but the degree of each metabolite formed by individual isozyme varied. Among the six CYP isozymes tested, CYP 1A2 and 2D6 were most active on catalyzing the metabolism of BPR0L075 that were followed by 2C19 and 3A4. CYP 2C9 and 2E1 were least active on catalyzing the metabolism of BPR0L075. While all six isozymes were capable of catalyzing the formation of the six identified metabolites, CYP 1A2 catalyzed mainly the formation of M1, M2 and M3. Whereas, M2 was the major metabolite of CYP 2D6 and M2 and M4 were the major metabolites of CYP 2C19 and 3A4.

Kinetic Analysis of BPR0L075 Metabolism

M2 (6-desmethyl-BPR0L075), the major metabolite of BPR0L075 identified in the mouse, rat, dog and human liver microsomal incubations, has also been shown to have cytotoxic activities against several human cancer cell lines but was less potent

DMD Fast Forward. Published on April 2, 2007 as DOI: 10.1124/dmd.106.014597
This article has not been copyedited and formatted. The final version may differ from this version.

than BPR0L075 (Liou et al., 2004). Thus, it is of important to determine the extent and the rate of BPR0L075 conversion to M2 in the liver microsomes of the four species. Table 2 and Figure 7 show the kinetic data of BPR0L075 to M2 metabolism in the liver microsomes of the four species. The Km and Vmax values for the metabolism of BPR0L075 to M2 were evaluated by Michaelis-Menton and Lineweaver-Burk plots (Figure 7). The calculated Km values were 3.4, 14.8, 50.1 and 26.7 μM, respectively, for mouse, rat, dog and human liver microsomes. The corresponding values for Vmax were 465, 512, 295 and 415 pmol/mg protein/min, respectively. The intrinsic clearance rates (Vmax/Km) for the conversion of BPR0L075 to M2 were 137, 34.6, 5.9 and 19.3 μL/mg protein/min, respectively, for mouse, rat, dog and human liver microsomes. The rank order of intrinsic clearance was mouse > rat > human > dog.

Conclusion

Six metabolites of BRP0L075 in the liver microsomal incubations of mouse, rat, dog and human were tentatively identified by LC-MS/MS as the products derived from hydroxylation on the indole ring (M1, M3 and M5) and O-demethylation (M2, M4 and M6). The structures of five metabolites were confirmed by comparing with the synthetic standards. The structure of one metabolite (M3) had not been identified due to lack of reference standard. Metabolite M2 (6-desmethyl-BPR0L075) was the major metabolite in all four species. No qualitative species-difference on the metabolism of BPR0L075 was observed. There was quantitative species-difference on the metabolism of BPR0L075 among the four species. The rank order of intrinsic clearance rates for the conversion of BPR0L075 to 6-desmethyl-BPR0L075 was mouse>rat>human>dog. Incubation of BPR0L075 with baculovirus-insect cell-expressed human CYP isozymes showed that CYP 1A2, 2C9, 2C19, 2D6, 2E1

DMD Fast Forward. Published on April 2, 2007 as DOI: 10.1124/dmd.106.014597
This article has not been copyedited and formatted. The final version may differ from this version.

and 3A4 all catalyzed the O-demethylation and hydroxylation of BPR0L075. CYP 1A2 and 2D6 were most active on catalyzing the metabolism of BPR0L075. CYP 1A2 catalyzed mainly the formation of M1, M2 and M3. CYP 2D6 catalyzed predominantly the formation of M2.

.

.

REFERENCES

Kuo CC, Hsieh HP, Pan WY, Chen CP, Liou JP, Lee SJ, Chang YL, Chen LT, Chen CT, Chang JY (2004) BPR0L075, a novel synthetic indole compound with antimitotic activity in human cancer cells, exerts effective antitumoral activity in vivo. *Cancer Res* 64:4621-4628.

Kerns EH (2001) High throughput physicochemical profiling for drug discovery. J Pharm Sci 90:1838-1858.

Hop CE, Tiller PR, Romanyshyn L (2002) In vitro metabolite identification using fast gradient high performance liquid chromatography combined with tandem mass spectrometry. Rapid Commun Mass Spectrom.16:212-219.

Liou JP, Chang YL, Kuo FM, Chang CW, Tseng HY, Wang CC, Yang YN, Chang JY, Lee SJ, Hsieh HP (2004) Concise synthesis and structure-activity relationships of combretastatin A-4 analogues, 1-aroylindoles and 3-aroylindoles, as novel classes of potent antitubulin agents. J Med Chem 47:4247-4257.

FOOTNOTE:

The authors are grateful to the National Health Research Institutes, Taiwan, Republic of China for financial support.

DMD Fast Forward. Published on April 2, 2007 as DOI: 10.1124/dmd.106.014597
This article has not been copyedited and formatted. The final version may differ from this version.

FIGURE LENGENDS

FIG. 1. The total ion and selectively extracted ion chromatograms of the acetonitrile extract of BPR0L075 incubated with human liver microsomes in the presence of NADPH.

FIG. 2. The MS/MS fragmentation patterns of BPR0L075 and its metabolites.

FIG. 3. The total ion and selectively extracted ion chromatograms of the acetonitrile extract of BPR0L075 incubated with mouse, rat, dog and human liver microsomes in the presence of NADPH.

FIG. 4. The HPLC/UV chromatograms of BPR0L075 and its metabolites in mouse, rat, dog and human liver microsomal incubations.

FIG. 5. The proposed metabolic schemes of BPR0L075 in mouse, rat, dog and human liver microsomes.

FIG. 6. The total ion and selectively extracted ion chromatograms of the acetonitrile extract of BPR0L075 incubated with six baculovirus-insect cell-expressed human CYP isozymes.

FIG. 7. Representative Michaelis-Menton plots and Lineweaver-Burk plots (insert) for the biotransformation of BPR0L075 to 6-desmethyl-BPR0L075 in mouse, rat, dog and human liver microsomes. Each point represents the mean of three determinations.

TABLE 1

The retention time, $[M+H]^+$ and major fragment ions and the relative percent distribution of metabolites identified in the incubation mixture of BPR0L075 in mouse, rat, dog and human liver microsomes.

Compound	Retention time (min)	$[M+H]^+$ ion m/z	Fragment ion 1 m/z	Fragment ion 2 m/z	% Distribution* (UV 286 nm)				Remark
					Mouse	Rat	Dog	Human	
M1	16.5	358	190	195	1.7 (4.0)**	1.5 (4.0)	2.5 (17.3)	2.1 (10.2)	Hydroxylation
M2	17.4	328	160	195	27.9 (66.4)	21.5 (56.9)	5.0 (34.7)	12.7 (61.7)	O-Demethylation
M3	18.7	358	190	195	0.5 (1.2)	0.7 (1.9)	1.3 (9.0)	3.0 (14.6)	Hydroxylation
M4	19.9	328	174	181	5.4 (12.9)	4.0 (10.6)	2.2 (15.3)	1.9 (9.2)	O-Demethylation
M5	21.7	358	190	195	0.3 (0.7)	0.1 (0.3)	1.4 (9.7)	0.3 (1.5)	Hydroxylation
M6	22.2	328	174	181	6.2 (14.8)	10.0 (26.5)	2.0 (13.9)	0.6 (2.9)	O-Demethylation
BPR0L075	28.5	342	174	195	58.0	62.1	85.7	79.3	Parent Compound

* These values are the approximate values estimated by UV absorption under the assumption that all metabolites have the same extinction coefficient of the parent compound at 286 nm. ** The values in parenthesis show the percent distribution of total metabolites formed.

DMD Fast Forward. Published on April 2, 2007 as DOI: 10.1124/dmd.106.014597
This article has not been copyedited and formatted. The final version may differ from this version.

TABLE 2

Kinetic parameters for BPR0L075 6-O-demethylation in mouse, rat, dog and human liver microsomes .

Species	K_m	V_{max}	V_{max} / K_m
	(μM)	(pmol/mg protein/min)	(μL/mg protein/min)
Mouse	3.4	465	137
Rat	14.8	512	34.6
Dog	50.1	295	5.9
Human	26.7	415	19.3

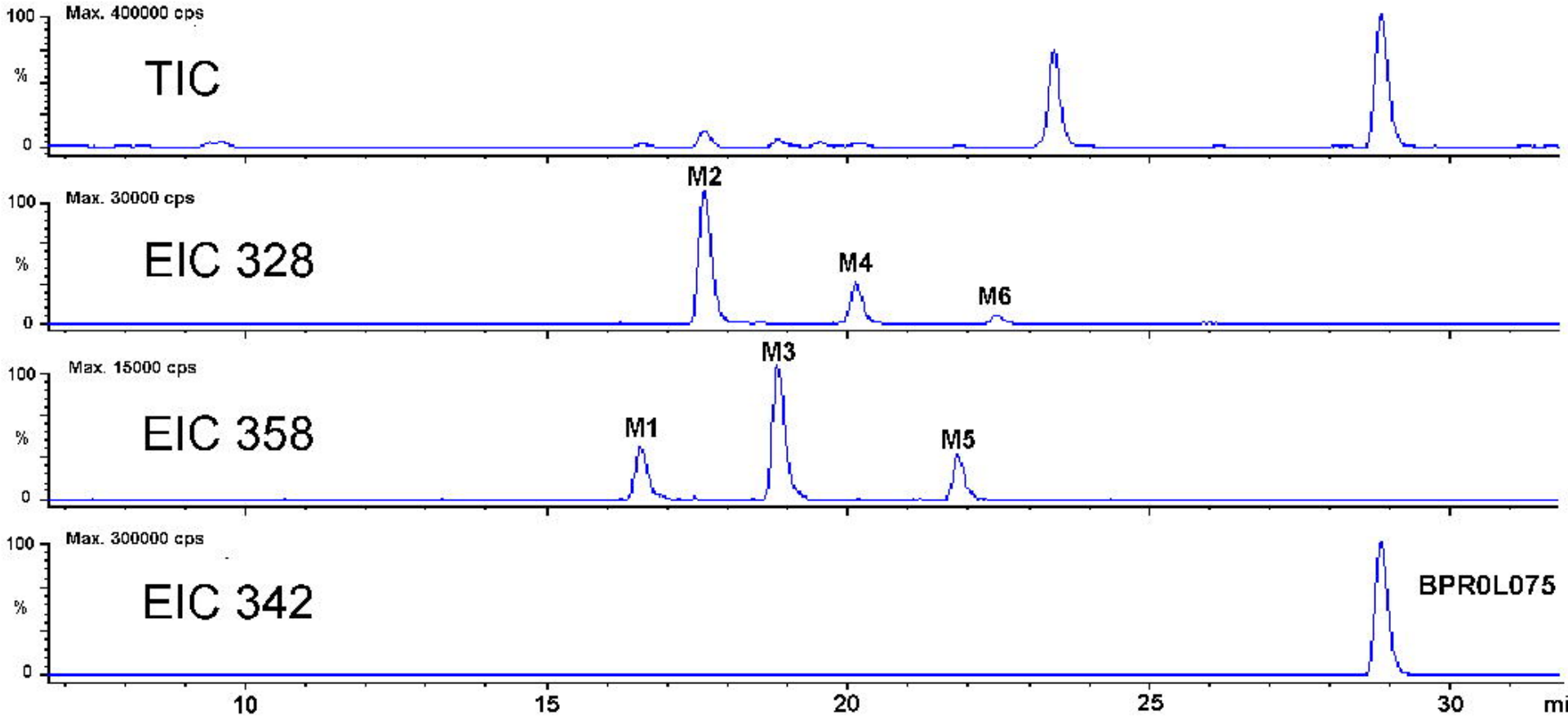
Max. 400000 cps
TIC
Max. 30000 cps
EIC 328
M2
M4
M6
Max. 15000 cps
EIC 358
M1
M3
M5
Max. 300000 cps
EIC 342
BPR0L075
100
%
0
10
15
20
25
30
min

Figure 1.

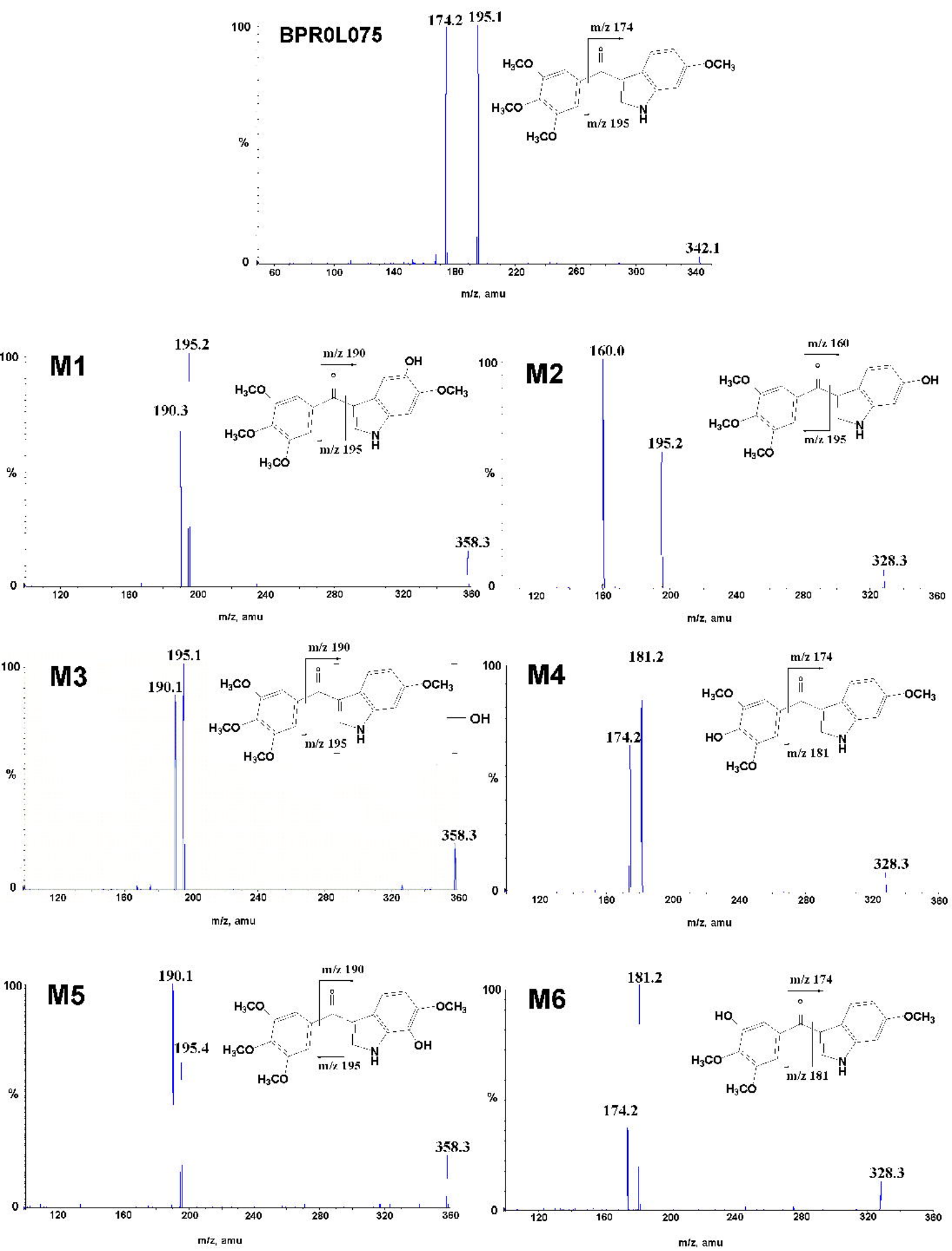
BPR0L075
174.2
195.1
342.1
m/z 174
m/z 195
m/z, amu
M1
195.2
190.3
358.3
m/z 190
m/z 195
M2
160.0
195.2
328.3
m/z 160
m/z 195
M3
195.1
190.1
358.3
m/z 190
m/z 195
M4
181.2
174.2
328.3
m/z 174
m/z 181
M5
190.1
195.4
358.3
m/z 190
m/z 195
M6
181.2
174.2
328.3
m/z 174
m/z 181

Figure 2.

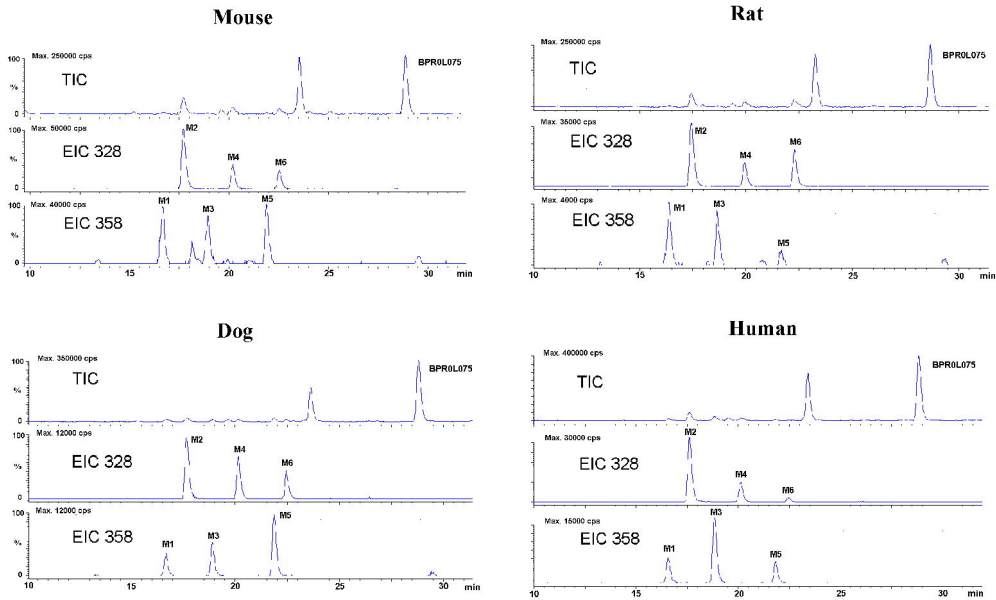
Mouse
Max. 250000 cps
TIC
BPR0L075
Max. 50000 cps
EIC 328
M2
M4
M6
Max. 40000 cps
EIC 358
M1
M3
M5
min
Rat
Max. 250000 cps
TIC
BPR0L075
Max. 35000 cps
EIC 328
M2
M4
M6
Max. 4000 cps
EIC 358
M1
M3
M5
min
Dog
Max. 350000 cps
TIC
BPR0L075
Max. 12000 cps
EIC 328
M2
M4
M6
Max. 12000 cps
EIC 358
M1
M3
M5
min
Human
Max. 400000 cps
TIC
BPR0L075
Max. 30000 cps
EIC 328
M2
M4
M6
Max. 15000 cps
EIC 358
M1
M3
M5
min

Figure 3.

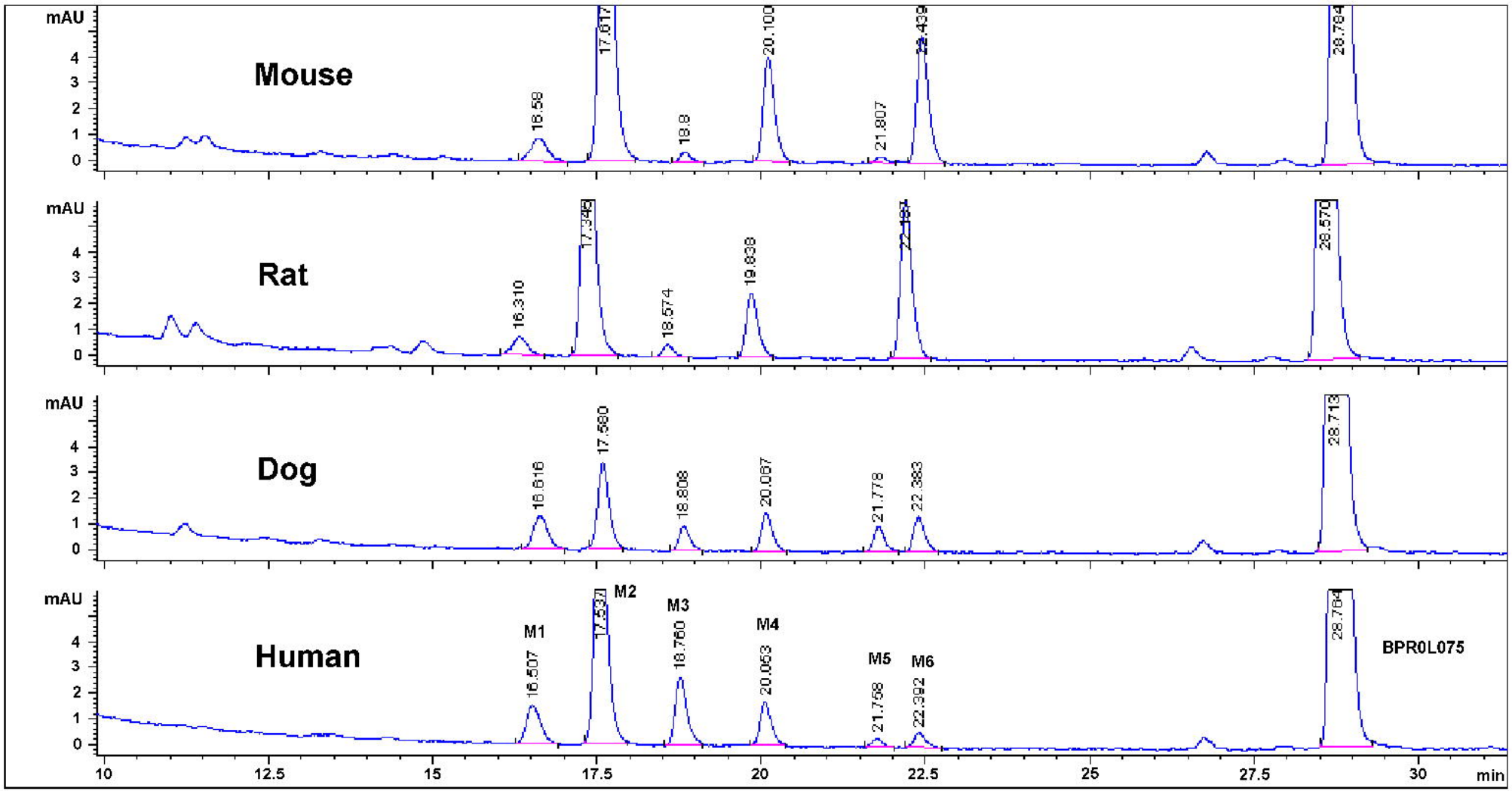
mAU
Mouse
16.58
17.617
18.8
20.100
21.807
22.439
28.784
mAU
Rat
16.310
17.345
18.574
19.838
22.187
28.570
mAU
Dog
16.616
17.580
18.808
20.067
21.778
22.383
28.713
mAU
Human
M1
M2
M3
M4
M5
M6
16.507
17.537
18.760
20.053
21.758
22.392
28.764
BPR0L075
10
12.5
15
17.5
20
22.5
25
27.5
30
min

Figure 4.

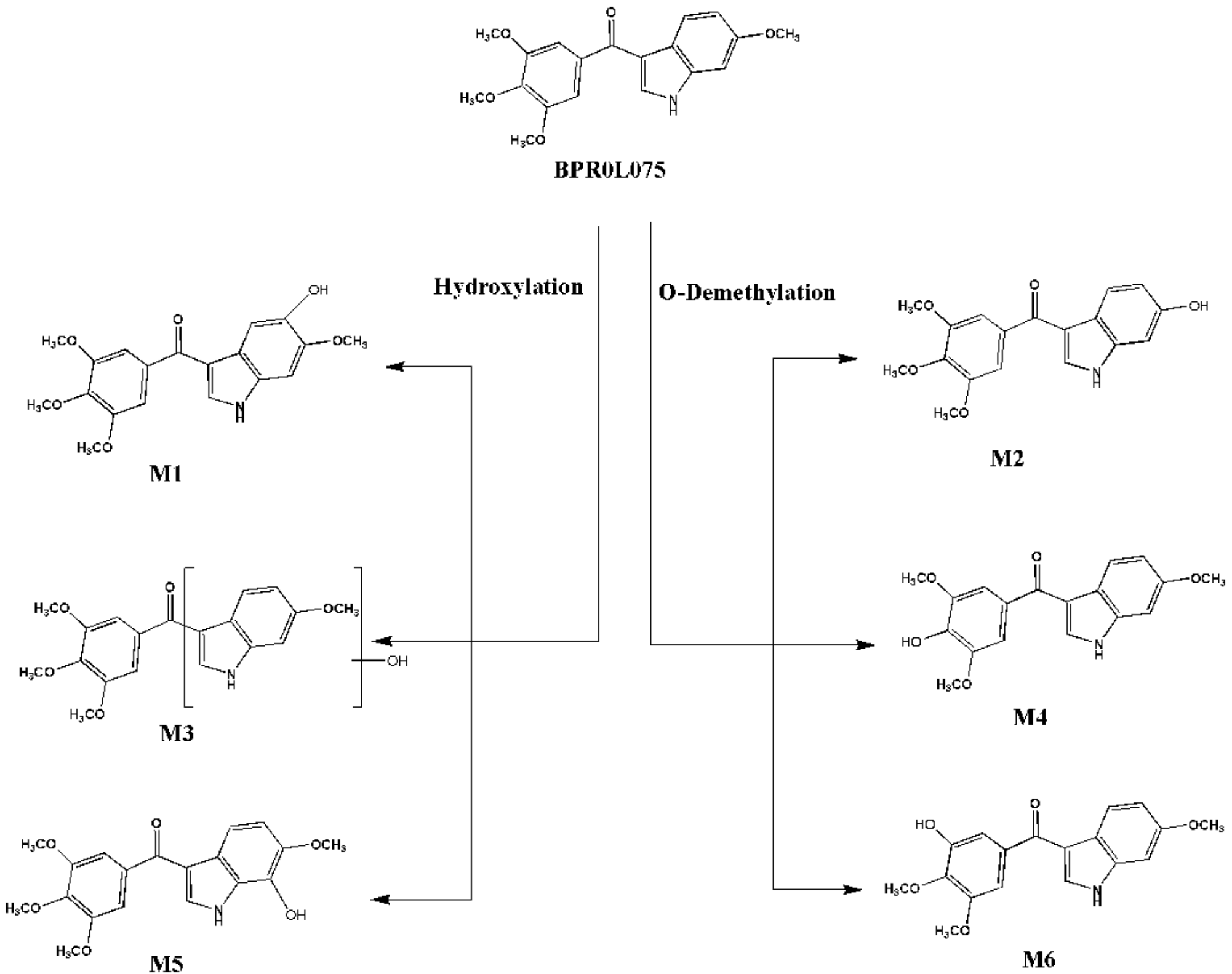

Figure 5.

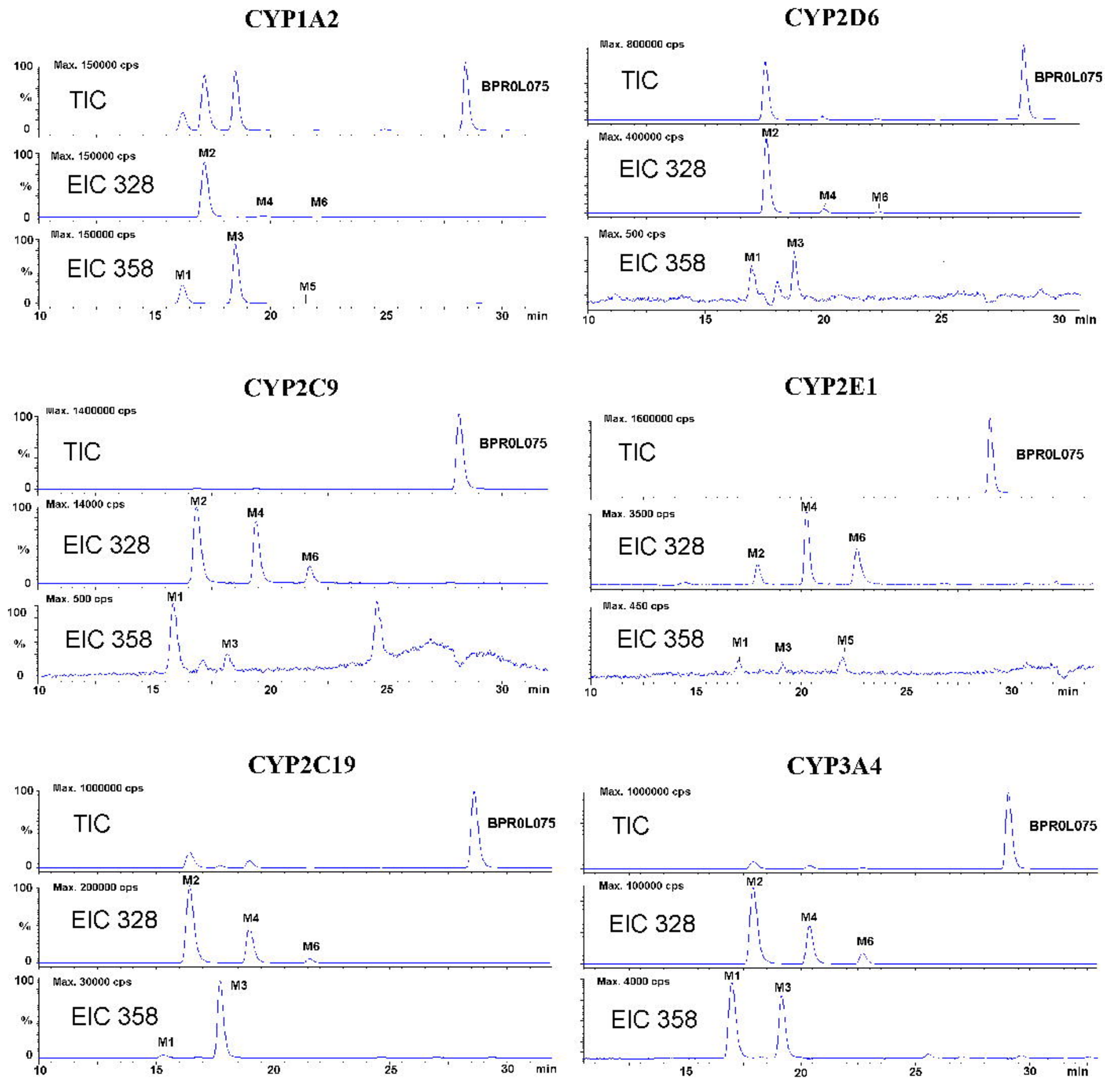
CYP1A2
Max. 150000 cps
TIC
BPR0L075
Max. 150000 cps
EIC 328
M2
M4
M6
Max. 150000 cps
EIC 358
M1
M3
M5
CYP2D6
Max. 800000 cps
TIC
BPR0L075
Max. 400000 cps
EIC 328
M2
M4
M6
Max. 500 cps
EIC 358
M1
M3
CYP2C9
Max. 1400000 cps
TIC
BPR0L075
Max. 14000 cps
EIC 328
M2
M4
M6
Max. 500 cps
EIC 358
M1
M3
CYP2E1
Max. 1600000 cps
TIC
BPR0L075
Max. 3500 cps
EIC 328
M2
M4
M6
Max. 450 cps
EIC 358
M1
M3
M5
CYP2C19
Max. 1000000 cps
TIC
BPR0L075
Max. 200000 cps
EIC 328
M2
M4
M6
Max. 30000 cps
EIC 358
M1
M3
CYP3A4
Max. 1000000 cps
TIC
BPR0L075
Max. 100000 cps
EIC 328
M2
M4
M6
Max. 4000 cps
EIC 358
M1
M3
min

Figure 6.

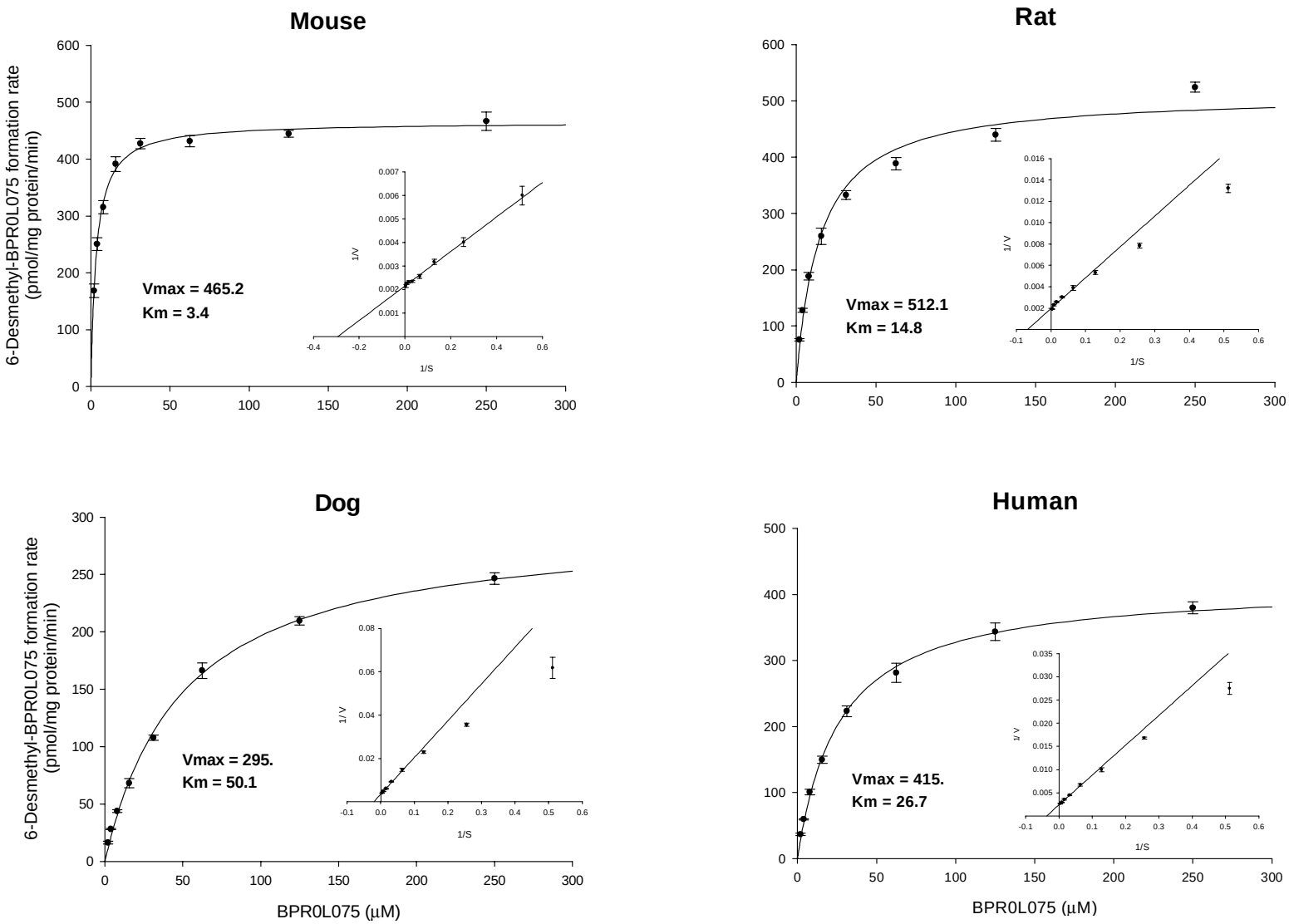

Figure 7.